

## Distribution and Organization of Auxotrophic Genes on the Multichromosomal Genome of *Burkholderia multivorans* ATCC 17616

Harunobu Komatsu, Yoshiyuki Imura, Akira Ohori, Yuji Nagata, and Masataka Tsuda\*

*Department of Environmental Life Sciences, Graduate School of Life Sciences, Tohoku University, Sendai 980-8577, Japan*

Received 4 December 2002/Accepted 12 March 2003

**The *Burkholderia multivorans* strain ATCC 17616 carries three circular chromosomes with sizes of 3.4, 2.5, and 0.9 Mb. To determine the distribution and organization of the amino acid biosynthetic genes on the genome of this  $\beta$ -proteobacterium, various auxotrophic mutations were isolated using a Tn5 derivative that was convenient not only for the determination of its insertion site on the genome map but also for the structural analysis of the flanking regions. Analysis by pulsed-field gel electrophoresis revealed that 20 out of 23 insertion mutations were distributed on the 3.4-Mb chromosome. More detailed analysis of the *his*, *trp*, *arg*, and *lys* mutations and their flanking regions revealed the following properties of these auxotrophic genes: (i) all nine *his* genes were clustered on the 3.4-Mb chromosome; (ii) seven *trp* genes were organized within two distinct regions, i.e., a *trpEGDC* cluster on the 3.4-Mb chromosome and a *trpFBA* cluster on the 2.5-Mb chromosome; (iii) the *leu* gene cluster, *leuCDB*, was also located close to the *trpFBA* cluster; and (iv) *lysA* and *argG* genes were located on the 2.5-Mb chromosome, in contrast to the *argH* gene, which was located on the 3.4-Mb chromosome. Southern hybridization analysis, allelic exchange mutagenesis of ATCC 17616, and complementation tests demonstrated that all of the genes examined were functional and existed as a single copy within the genome. The present findings also indicated that the 2.5-Mb chromosome carried various auxotrophic genes with no structural or functional counterparts on the remaining two chromosomes.**

The *Burkholderia cepacia* complex (Bcc) consists of several species of closely related and aerobic bacteria belonging to the  $\beta$  subgroup of *Proteobacteria*, and they are ubiquitously distributed in various natural environments (9, 27). Due to their production of various antifungal metabolites and extraordinary biodegradative abilities, some strains within this complex have shown great potential for application in the biocontrol of soil-borne plant pathogens and for the bioremediation of polluted environments. Other strains within this complex have been recognized as plant pathogens and as serious opportunistic pathogens of humans with cystic fibrosis (21, 27). The Bcc complex has an unusually complex genome, and almost all examined Bcc strains have three large (>600 kb) circular replicons (most probably chromosomes) with total genome sizes of >7 Mb (21, 30). The genomes of some strains have exhibited frequent and large-scale rearrangements, including the deletion and translocation of a part of one chromosome to another (21).

One strain, ATCC 17616, belonging to genomovar II of the Bcc, has recently been designated *B. multivorans* (38). This strain has been reported to show genome rearrangements that are probably due to the high degree of transposition activity exhibited by a number of its insertion elements (4, 14, 21). As shown in Fig. 1, this strain has been reported to carry three circular chromosomes of 3.4, 2.5, and 0.9 Mb in size (hereafter designated Chr I, Chr II, and Chr III, respectively), each con-

taining at least one copy of the rRNA gene (7). The genome map of ATCC 17616 has been constructed by use of three rare-cutting restriction enzymes, *PacI*, *PmeI*, and *SwaI*. To date, however, the genetic organization of the three chromosomes has remained poorly characterized, and only four auxotrophic and three catabolic genes have been mapped on the genome (i.e., the *arg*, *ile*, and *his* genes on Chr I and a *lys* gene and the genes for the catabolism of ribitol, trehalose, and phthalate on Chr II) (8). A more detailed characterization of the organization of these genes and their flanking regions has until now remained a task for future study.

Based on molecular biological and genome sequence analyses, chromosome multiplicities have been recognized in other bacteria (1, 19, 25, 35, 37, 40, 42). In bacteria containing two chromosomes, the larger chromosome usually carries almost all of the essential housekeeping genes and the genes coding for primary metabolic enzymes such as those required for amino acid biosynthesis. In contrast, the smaller chromosome tends to contain second and/or third genes that have counterparts on the larger chromosome (7, 11, 15–17, 31, 39). However, there are several exceptions. For example, *Rhodobacter sphaeroides* 2.4.1 was experimentally shown to carry two functional tryptophan biosynthetic genes (i.e., *trpB* and *trpF*) on only the smaller chromosome (23), whereas the smaller (2.1-Mb) chromosome (designated a megaplasmid in reference 31) of a  $\beta$ -proteobacterium, *Ralstonia solanacearum* GMI1000, has been thought to carry some amino acid biosynthetic genes (e.g., *metB* and *metE*) with no counterparts on the larger (3.7-Mb) chromosome.

The aim of the present study was to gain additional experimental understanding of the distribution and organization of

\* Corresponding author. Mailing address: Department of Environmental Life Sciences, Graduate School of Life Sciences, Tohoku University, 2-1-1 Katahira, Sendai 980-8577, Japan. Phone and fax: 81-22-217-5699. E-mail: mtsuda@ige.tohoku.ac.jp.

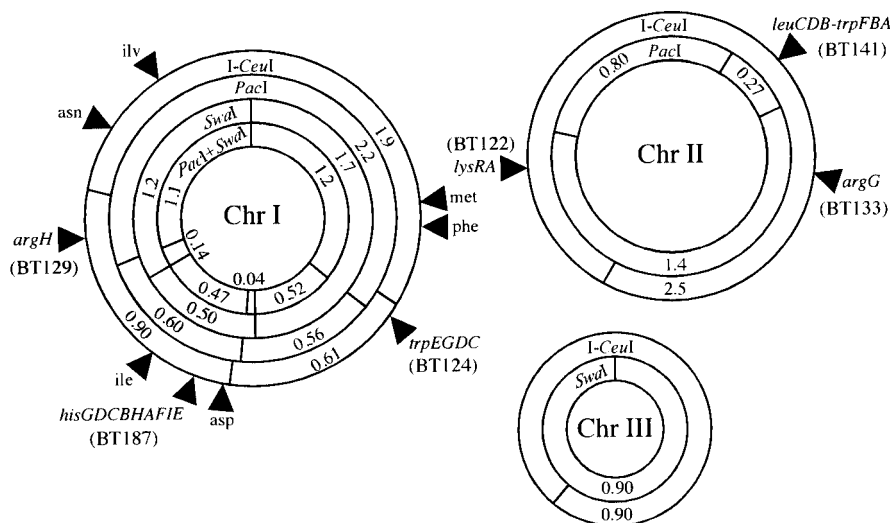


FIG. 1. Genome map of *B. multivorans* ATCC 17616. The numbers shown with the restriction fragment designations are the sizes in megabases. Note that Chr II and Chr III lack the *SwaI* and *PacI* sites, respectively (8). Arrowheads indicate the positions of the auxotrophic genes identified in this study. The PFGE mapping of the TnMod-RTp' insertion sites in the BT strains whose designations are shown in parentheses are described in detail in the text and in the legend to Fig. 3.

the amino acid biosynthetic genes on the *B. multivorans* ATCC 17616 genome. For this purpose, we obtained various auxotrophic mutations by insertion of a 1.2-kb mini-Tn5 derivative, TnMod-RTp' (Fig. 2), which enabled us to achieve the following goals: (i) clarification of the function of the mutated gene, (ii) determination of the position of the insertion site on the genome map, and (iii) cloning and analysis of the flanking regions of the insertion site (12). The results indicated that (i) the majority of the auxotrophic genes were present on Chr I and (ii) functional auxotrophic genes such as *argG*, *leuCDB*, *lysA*, and *trpFBA* were located on Chr II with no counterparts on the remaining two chromosomes.

MATERIALS AND METHODS

**Bacterial strains, plasmids, and media.** The bacterial strains and plasmids used in this study are listed in Table 1. *Escherichia coli* and *B. multivorans* cells were cultivated at 37 and 26°C, respectively. Liquid media used were M9 minimal medium containing 0.2% succinate as a carbon source and Luria broth (LB) (3). Solid media were prepared by the addition of 1.5% agar. When needed, isopro-

pyl-β-D-thiogalactopyranoside and 5-bromo-4-chloro-3-indolyl-β-D-galactopyranoside were used at final concentrations of 0.5 mM and 40 μg/ml, respectively. Selective agents added to the media were as follows: ampicillin (Ap) at 50 μg/ml for *E. coli*, kanamycin (Km) at 50 μg/ml for *E. coli* and 150 μg/ml for *B. multivorans*, tetracycline (Tc) at 10 μg/ml for *E. coli* and 50 μg/ml for *B. multivorans*, and trimethoprim (Tp) at 250 μg/ml for *E. coli* and 100 μg/ml for *B. multivorans*.

**Basic DNA manipulation.** Established protocols were used for the following procedures: preparation of genomic and plasmid DNA, DNA digestion with restriction endonucleases, ligation, standard agarose gel electrophoresis, and transformation of *E. coli* cells (32). Transformation of *B. multivorans* cells was carried out by electroporation. *B. multivorans* cells grown to an optical density at 600 nm of 0.6 were collected by centrifugation and washed three times with a half-volume of ice-cold 1 mM MOPS buffer containing 10% glycerol. The cells were then pelleted by centrifugation for 10 min at 3,000 × g and resuspended in a 0.01 vol of the buffer to obtain a concentration of about 1 × 10<sup>10</sup> cells/ml. A 100-μl aliquot of the cell suspension and plasmid DNA was transferred to an ice-cold electroporation cuvette (Bio-Rad; 2-mm-wide gap) and pulsed using a Gene Pulser (Bio-Rad) at 2.5 kV, 25 μF, and 400 Ω. After electroporation, the cells were incubated for 4 h in 1 ml of LB containing 10% glycerol and plated on LB agar plates containing the appropriate antibiotics.

PCR was performed with *ExTaq* DNA polymerase (TaKaRa, Kyoto, Japan). PCR amplification of a portion of the 16S rRNA gene from the ATCC 17616 genome was performed with primers 5'-AGAGTTTGATCTGGCTCAG-3' and 5'-AAGGAGGTGATCCRCGCA-3' (2). The 0.36-kb fragment carrying a part of the ATCC 17616 *trpB* gene was amplified with the degenerated primers 5'-GGNGGNGNWSNAAYGCN-3' and 5'-YTCNARNCGNGDATDATNCCYTC-3' (26).

**PFGE.** An agarose block containing the unsharred genomic DNA was prepared as described by Cheng and Lessie (8). Before digestion of DNA with restriction endonuclease, an appropriate amount of the agarose block was transferred into a 1.5-ml Eppendorf tube and equilibrated three times with 1 ml of the restriction buffer for 30 min at 4°C (29). After replacement of this buffer with 0.2 ml of fresh restriction buffer, the agarose block was treated for 2 h with 10 U of *PacI*, *I-CeuI*, or *SwaI* at 37°C (for *PacI* and *I-CeuI*) or at 25°C (for *SwaI*). Using the CHEF DR III system (Bio-Rad), the DNA fragments ranging from 50 kb to 1.4 Mb in size were separated by pulsed-field gel electrophoresis (PFGE) through 1% pulsed-field certified agarose (Bio-Rad) in 0.5× Tris-borate buffer (45 mM Tris-HCl, 45 mM boric acid, 1 mM EDTA, pH 8.0) at 14°C and 6 V cm<sup>-1</sup>. The pulse times were 10 to 40 s for 24 h and 15 to 160 s for 28 h for the separation of the fragments ranging in size from 50 kb to 600 kb and from 250 kb to 1.4 Mb, respectively. To clearly separate the fragments of more than 1.4 Mb in size, PFGE was carried out with pulse times of 120 to 360 s for 42 h through 0.8%

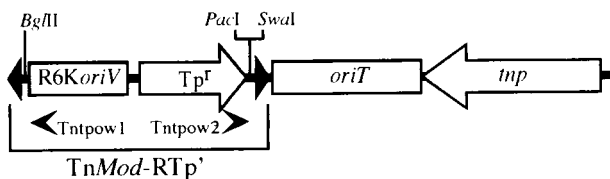


FIG. 2. Linearized map of pTnMod-RTp'. The figure is drawn schematically (12). The arrows represent the transcriptional directions of the *Tp<sup>I</sup>* and transposase (*trp*) genes. The boxes represent the R6K origin of replication (*R6KoriV*) and the RP4-derived origin of transfer (*oriT*). The supply in *trans* of  $\pi$  protein (*pir* gene product) and the RP4-specified transfer function allowed vegetative replication and conjugal mobilization, respectively, of pTnMod-RTp' (34). The black triangles represent inverted repeats. The arrowheads below the map indicate the positions of the primers (Tntpow1 and Tntpow2) used for DNA sequencing.

TABLE 1. Bacterial strains and plasmids used in this study

Strain or plasmid	Relevant characteristic(s)	Reference or source
<b>Strains</b>		
<i>E. coli</i>		
DH5 $\alpha$	<i>recA1 endA1 gyrA96 thi-1 hsdR17 supE44</i> $\Delta$ ( <i>lac</i> )U169 ( $\phi$ 80d <i>lac</i> $\Delta$ M15)	3
XL1-Blue MR	$\Delta$ ( <i>mcrA</i> )183 $\Delta$ ( <i>mcrCB-hsdSMR-mrr</i> )173 <i>endA1 supE44 thi-1 recA1 gyrA96 relA1 lac</i>	Stratagene
S17-1	<i>thi pro recA hsdR</i> Tp <sup>r</sup> Sm <sup>r</sup> ; chromosomally integrated RP4-Tc::Mu-Km::Tp7	34
JM109( $\lambda$ pir)	$\lambda$ pir lysogen of JM109	Lab collection
<i>B. multivorans</i>		
ATCC 17616	Soil isolate; genomovar II of the Bcc	ATCC <sup>b</sup>
BT141	ATCC 17616::Tn <i>Mod</i> -RTp <sup>r</sup> ; leaky Trp <sup>-</sup>	This study
BT211	ATCC 17616 <i>leuD::kan<sup>r</sup></i> ; knockout mutant by use of pKOM154	This study
BT214	ATCC 17616 $\Delta$ ( <i>trpF-B</i> ): <i>kan</i> ; knockout mutant by use of pKOM157	This study
BT216	ATCC 17616 with the insert of the Tn <i>Mod</i> -RTp <sup>r</sup> - $\Omega$ <i>kan</i> cassette from pKOM160	This study
<b>Plasmids</b>		
pTn <i>Mod</i> -RTp <sup>r</sup>	Tp <sup>r</sup> ; Tn <i>Mod</i> -RTp <sup>r</sup> -containing plasmid whose transposable region containing the Tp <sup>r</sup> gene, R6 <i>KoriV</i> , and <i>PacI</i> and <i>SwaI</i> sites is able to transpose by the transposase that is encoded outside of the Tn <i>Mod</i> -RTp <sup>r</sup> region	12
pUC18	Ap <sup>r</sup> ; cloning vector	41
pUC19	Ap <sup>r</sup> ; cloning vector	41
pUC4K	Km <sup>r</sup> Ap <sup>r</sup> ; <i>kan</i> flanked by inverted repeats of oligonucleotide containing <i>SalI</i> and <i>PstI</i> sites	36
pEX18Tc	Tc <sup>r</sup> <i>sacB oriT</i> ; suicide vector for gene replacement carrying the pUC18-derived multiple cloning sites	18
pHP45 $\Omega$ Km	Ap <sup>r</sup> Km <sup>r</sup> ; $\Omega$ <i>kan</i> flanked by transcription terminators and <i>BamHI</i> sites	13
pBBR1MCS	Cm <sup>r</sup> ; broad-host-range cloning vector	20
SuperCos1	Ap <sup>r</sup> Km <sup>r</sup> ; cosmid vector	Stratagene
pSBm1-92	SuperCos1 derivative carrying the <i>trpB</i> region of ATCC 17616	This study
pBTB141	Tp <sup>r</sup> ; Tn <i>Mod</i> -RTp <sup>r</sup> -containing plasmid recovered by self-ligation of the <i>BamHI</i> -treated genome of BT141	This study
pKOM152	pEX18Tc derivative carrying the <i>BamHI</i> -linearized form of pBTB141	This study
pKOM154	pEX18Tc derivative with the pKOM152-derived, <i>leuD</i> -containing <i>BamHI</i> - <i>EcoRI</i> fragment that has the insert of the pUC4K-derived <i>kan</i> in <i>leuD</i>	This study
pKOM157	pEX18Tc derivative with the <i>trpFB</i> -containing <i>BamHI</i> fragment in which the <i>XhoI</i> fragment containing these genes is replaced by the <i>SalI</i> -flanked <i>kan</i> from pUC4K	This study
pKOM159	pEX18Tc derivative with the Tn <i>Mod</i> -RTp <sup>r</sup> -containing <i>EcoRI</i> fragment from pKOM152	This study
pKOM160	pKOM159 derivative in which the Tn <i>Mod</i> -RTp <sup>r</sup> -derived <i>BglII</i> site has the insert of the <i>BamHI</i> -flanked $\Omega$ <i>kan</i> from pHP45 $\Omega$ Km	This study

<sup>a</sup> *kan*, Km<sup>r</sup> gene.

<sup>b</sup> ATCC, American Type Culture Collection.

agarose in 1 $\times$  TAE buffer (40 mM Tris-HCl, 40 mM acetate, 1 mM EDTA, pH 8.0) at 14 $^{\circ}$ C and at 4 V cm<sup>-1</sup>. The size of migrated DNA fragments was estimated based on *Saccharomyces cerevisiae* chromosomal DNA (Bio-Rad), which was used as a standard.

**Southern hybridization.** Using the established protocols (28), Southern hybridization analysis was carried out. The DNA fragments separated by gel electrophoresis were transferred onto a Hybond-N nylon membrane (Amersham Biosciences) by capillary transfer (29). Using a GS GENE LINKER UV chamber (Bio-Rad) before transfer, the large DNA fragments separated by PFGE were nicked by UV. Using a DIG (digoxigenin) DNA labeling kit (Roche Diagnostics), the probe DNA fragment was labeled with DIG, and the hybridized DNA fragment was detected by a DIG DNA detection kit (Roche Diagnostics).

**Transposon and allelic exchange mutagenesis.** To obtain *B. multivorans* mutants that were auxotrophic for various amino acids, we employed Tn*Mod*-RTp<sup>r</sup>, a 1.2-kb Tn5 derivative containing the *PacI* and *SwaI* sites at one extreme end (Fig. 2) (12). A 3- $\mu$ g portion of pTn*Mod*-RTp<sup>r</sup> was used to transform the ATCC 17616 cells by electroporation, and the Tp<sup>r</sup> colonies selected on LB agar plates were checked for growth on M9 succinate minimal agar plates. Using pEX18Tc, a ColE1-based vector carrying the *sacB* gene and the RP4-derived *oriT* region (34), allelic exchange mutagenesis of the *B. multivorans* genome was carried out by the method of Hoang et al. (18). The ATCC 17616 DNA fragment with an insert of the Tp<sup>r</sup> or Km<sup>r</sup> gene was cloned into pEX18Tc, and the resulting plasmid was mobilized conjugally from an *E. coli* strain, S17-1 (33), to ATCC 17616. The transconjugants were selected on Tp- or Km-containing M9 minimal agar plates supplemented with 5% sucrose and an appropriate amino acid(s). The genomic DNA of the transconjugants that were sensitive to Tc was analyzed by Southern hybridization to confirm the allelic exchange.

**Construction of plasmids.** The SuperCos1-based cosmid library of the ATCC 17616 genome was constructed by partial digestion of the genomic DNA with *Sau3AI*, ligation with the *BamHI*-treated SuperCos1, in vitro packaging with Gigapack Gold III packaging extracts (Stratagene), and transfection of XL1-Blue MR.

pBTB141 was the 8.2-kb R6*KoriV*-driven plasmid that was recovered in JM109( $\lambda$ pir) by self-ligation of the *BamHI*-treated genome of BT141 (see Fig. 4C). The *BamHI*-linearized form of this plasmid was inserted into the *BamHI* site of pEX18Tc to construct pKOM152 such that the *BamHI* site in *truA* was located adjacent to the vector-derived *EcoRI* site. The Tn*Mod*-RTp<sup>r</sup>-containing *EcoRI* fragment of pKOM152 was recombined into the *EcoRI* site of pEX18Tc to obtain pKOM159. The *BamHI*-flanked  $\Omega$ Km cassette from pHP45 $\Omega$ Km (13) was next inserted at the *BglII* site that was located at one end of the transposon (Fig. 2) on pKOM159, and the resulting plasmid was designated pKOM160. The *BamHI*-*EcoRI* fragment containing the *leuD* gene (see Fig. 4C) was excised from pKOM152 and inserted into the corresponding sites of pEX18Tc, and the *PstI* site in the *leuD* gene of the resulting plasmid was subjected to insertion of the pUC4K-derived, *PstI*-flanked Km<sup>r</sup> gene to generate pKOM154. The *trpFB*-containing *BamHI* fragment from pSBm1-92 (see Fig. 4C) was inserted into the *BamHI* site of pEX18Tc, and the *XhoI* fragment covering the *trpF* and *trpB* genes on the resulting plasmid was replaced by the pUC4K-derived *SalI*-flanked Km<sup>r</sup> gene to construct pKOM157.

To complement the auxotrophic mutations on the genome, the genomic DNA fragments carrying the wild-type alleles were inserted into the multiple cloning sites of pBBR1MCS (20) such that the inserted genes were able to be transcribed from the vector-derived *lac* promoter. Details of the procedures used to construct the pBBR1MCS-based plasmids (see Fig. 4) are available upon request.

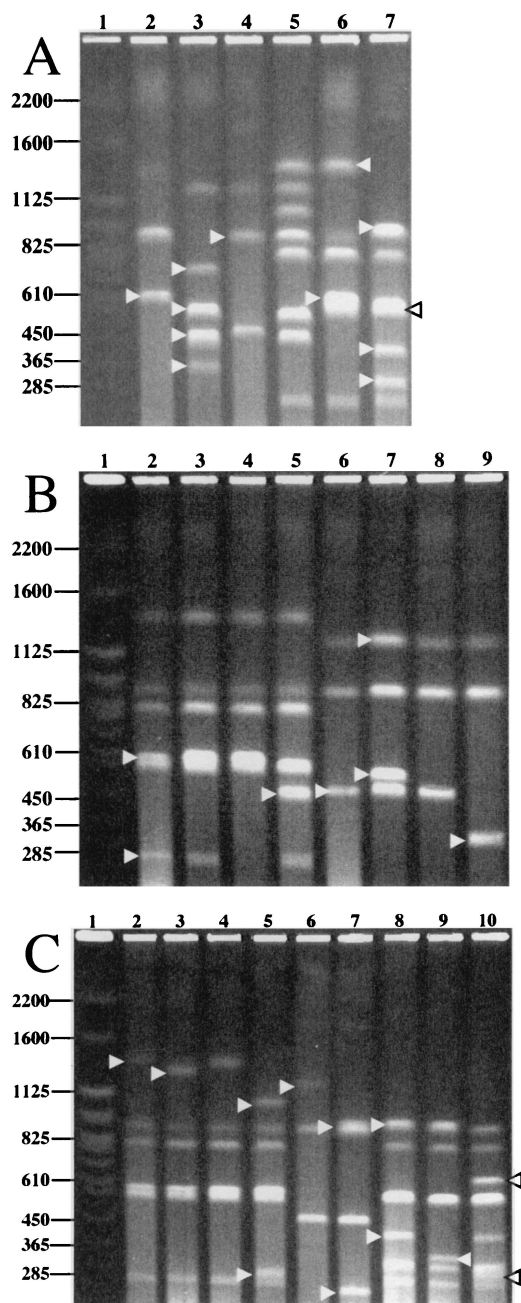


FIG. 3. PFGE mapping of the I-CeuI sites and the TnMod-RTp' insertion sites on the genome of ATCC 17616. Restriction patterns determined by PFGE assays whose running conditions were suitable to separate clearly the DNA fragments ranging in size from 250 kb to 1.4 Mb are depicted. The restriction patterns clearly demonstrating the presence of fragments more than 1.4 Mb and less than 250 kb in size are not shown; they can be provided upon request. The *S. cerevisiae* chromosomes were applied as size standards in lane 1 of each of the three panels, and the sizes are indicated in kilobases. The DNA fragments described in the text are marked by arrowheads. (A) Mapping of the I-CeuI sites on the ATCC 17616 genome. The following enzymes were used to digest the ATCC 17616 genome: lane 2, I-CeuI; lane 3, I-CeuI plus *Swa*I; lane 4, *Swa*I; lane 5, *Swa*I plus *Pac*I; lane 6, *Pac*I; and lane 7, *Pac*I plus I-CeuI. (B) Mapping the TnMod-RTp' insertion sites in Trp<sup>-</sup> and His<sup>-</sup> mutants. Lanes 2 and 6, ATCC 17616; lanes 3 and 7, BT124 (*trpG*); lanes 4 and 8, BT141 (a leaky Trp<sup>-</sup> mutant); lanes 5 and 9, BT187 (*hisA*). The genomes were digested by *Pac*I (lanes 2 to 5) and *Swa*I (lanes 6 to 9). (C) Mapping of the TnMod-RTp' insertion

These plasmids were introduced into the auxotrophic mutants of ATCC 17616 by electroporation.

**Nucleotide sequence accession numbers.** Cloned DNA fragments were sequenced by using an ABI PRISM 310 sequencer (Applied Biosystems) with universal, reverse, and custom-synthesized primers. The two primers Tntpow1 (5'-TTAACGCTGACATGGGGGGGT-3') and Tntpow2 (5'-TTGAACGTG TGGCCTAAGCGAGC-3') were employed for determination of the ATCC 17616 sequences located adjacent to the R6*KoriV*' and Tp<sup>r</sup> ends, respectively, of the TnMod-RTp' insert (Fig. 2). The nucleotide and protein sequences were analyzed by using Genetyx 11 software (SDC Inc., Tokyo, Japan). Sequence homologies were analyzed by the BLAST 2.0 programs (National Institute of Genetics, Mishima, Japan) (24). The nucleotide sequences described in this paper have been deposited in the DDBJ/EMBL/GenBank databases under the following accession numbers: AB091436 (for the 8.5-kb region containing the nine *his* genes), AB091305 (for the 7.5-kb region containing the *trpEGDC* cluster), AB091435 (for the 13-kb region containing the *leuCDB* and *trpFBA* clusters), AB091437 (for the 3.7-kb region containing *argH*), AB091438 (for the 5.4-kb region containing *argG*), AB092607 (for the 3.0-kb region containing *lysA*), and AB092606 (for the 1.5-kb region covering a part of the 16S rRNA gene).

## RESULTS

**Mapping of *rrn* operons.** Cheng and Lessie (8) have demonstrated by Southern hybridization analysis that the ATCC 17616 genome carried the *rrn* operons in the 1.2-, 1.1-, and 0.47-Mb *Swa*I-*Pac*I fragments from Chr I, in the 1.4-Mb *Pac*I fragment from Chr II, and in Chr III (Fig. 1). However, the exact copy number and precise position of each *rrn* operon on the genome map remained unknown. Southern hybridization analysis of the *Xho*I-digested genomic DNA by use of the PCR-amplified fragment of the 16S rRNA gene as the probe revealed that ATCC 17616 carried five copies of the 16S rRNA gene (data not shown). Enzyme I-CeuI specifically digests the prokaryotic 23S rRNA gene (22), and digestion of the ATCC 17616 genome by I-CeuI generated five DNA fragments with sizes of 2.5, 1.9, 0.90, 0.90, and 0.61 Mb (Fig. 3A, lane 2). These results indicated that (i) each of the five DNA fragments reported by Cheng and Lessie (8) carried one copy of the *rrn* operon, (ii) Chr I consisted of the 1.9-, 0.90-, and 0.61-Mb I-CeuI fragments, and (iii) a single I-CeuI site was situated on both Chr II and Chr III. The I-CeuI site on Chr III was found to be located 0.34 Mb apart from a unique *Swa*I site, since the Chr III-derived 0.90-Mb *Swa*I fragment was converted into 0.56- and 0.34-Mb *Swa*I-I-CeuI fragments (Fig. 3A, lanes 3 and 4). The Chr II-derived 1.4-Mb *Pac*I fragment was divided into 0.96- and 0.44-Mb fragments by additional treatment with I-CeuI (Fig. 3A, lanes 6 and 7). Strain BT141 was an ATCC 17616 derivative in which a TnMod-RTp' insert was located in the middle of the 0.27-Mb *Pac*I fragment on Chr II (Fig. 3B, lanes 2 and 4) (see below), therefore giving this chromosome a novel *Swa*I site that had originated from TnMod-RTp'. Since Chr II of BT141 generated 1.4- and 1.1-Mb fragments by double digestion with I-CeuI and *Swa*I (data not shown), the I-CeuI site on Chr II was concluded to be located at the position 0.44 Mb counterclockwise from the 0.80-Mb *Pac*I fragment (Fig. 1). Double digestion of the ATCC 17616 genome with

sites in Lys<sup>-</sup> and Arg<sup>-</sup> mutants. Lanes 2, 6, and 8, ATCC 17616; lanes 3 and 9, BT122 (*lysA*); lanes 4 and 7, BT129 (*argH*); lanes 5 and 10, BT133 (*argG*). The genomes were digested by *Pac*I (lanes 2 to 5), *Swa*I (lanes 6 and 7), and *Pac*I plus I-CeuI (lanes 8 to 10).

TABLE 2. Summary of TnMod-RTp'-inserted mutants

Amino acid(s) for which mutant(s) is auxotrophic <sup>a</sup>	Mutant name(s) <sup>b</sup>
Histidine	BT111 <sup>#</sup> ( <i>hisB</i> ), BT187 <sup>#</sup> ( <i>hisA</i> ), BT185 <sup>#</sup> ( <i>hisF</i> ), BT148 <sup>#</sup> ( <i>hisE</i> ), BT154 ( <i>hisE</i> )
Tryptophan	BT169 <sup>#</sup> ( <i>trpE</i> ), BT188 <sup>#</sup> ( <i>trpE</i> ), BT172 <sup>#</sup> ( <i>trpE</i> ), BT124 <sup>#</sup> ( <i>trpG</i> ), BT116 <sup>*#</sup> ( <i>trpD</i> ), BT114 <sup>*</sup> ( <i>trpC</i> ), BT141 <sup>*</sup> ( <i>orf5</i> , leaky Trp <sup>-</sup> phenotype)
Arginine	BT129 ( <i>argH</i> ), BT133 <sup>*#</sup> ( <i>argG</i> )
Lysine	BT122 <sup>*#</sup> ( <i>lysA</i> )
Asparagine	BT155
Aspartate	BT107, BT135
Isoleucine	BT178, BT182
Isoleucine and valine	BT179
Methionine	BT151
Phenylalanine	BT138

<sup>a</sup> Amino acid(s) required for normal growth on M9 succinate minimal agar plates.

<sup>b</sup> The gene inserted by the transposon is indicated in parentheses. The auxotrophic mutations of the strains whose designations are marked by "\*" were proven to be due to the transposon insertion through construction of the pEX18Tc derivative with the insert of the TnMod-RTp'-containing chromosomal fragment and subsequent allelic exchange mutagenesis of ATCC 17616 by the resulting plasmid. The auxotrophic mutants whose designations are marked by "#" were complemented to prototrophy by the pBBR1MCS-based plasmid carrying the wild-type allele. Southern hybridization analysis under low-stringency conditions confirmed that each gene whose name is underlined is present in a single copy on the genome. See text and legends to Fig. 1 and 4 for details.

I-CeuI and *PacI* led to a loss of the Chr I-derived 2.2- and 0.6-Mb *PacI* fragments with concomitant generation of novel 0.32- and 0.58-Mb fragments, but the Chr I-derived 1.9-Mb I-CeuI and 0.56-Mb *PacI* fragments remained unchanged by this double digestion (Fig. 3A, lanes 2, 6, and 7). The Chr I-derived 1.2-Mb *SwaI* fragment was divided into 0.74- and 0.46-Mb fragments by additional digestion with I-CeuI (Fig. 3A, lane 3). These restriction patterns enabled the mapping of three I-CeuI sites on Chr I such that (i) one site was 0.32 Mb clockwise from the 0.60-Mb *PacI* fragment and (ii) the remaining two sites in the 0.60- and 2.2-Mb *PacI* fragments were very close (<50 kb) to both ends of the 0.56-Mb *PacI* fragment (Fig. 1).

**Transposon mutagenesis of ATCC 17616.** For the mutagenesis of ATCC 17616, we employed a plasmid, pTnMod-RTp', that carried (i) the Tp' gene, the vegetative replication origin of the *E. coli*-specific plasmid R6K, and the *PacI* and *SwaI* sites in the 1.2-kb TnMod-RTp' region and (ii) the transposase gene outside of the transposon (Fig. 2) (10). Electroporation of the ATCC 17616 cells with 1 µg of the plasmid DNA led to the formation of approximately 200 transformants on LB agar plates containing Tp. Southern hybridization analysis of six such arbitrarily chosen transformants indicated that (i) each genome carried only one copy of the TnMod-RTp' region with a concomitant loss of the remaining portion of the plasmid and (ii) the insertion sites differed among the transformants (data not shown).

Approximately 5,100 Tp<sup>r</sup> transformants were obtained independently, and the 44 derivatives failed to grow on M9 succinate minimal agar plates. Among these derivatives, the 23 mutants grew normally on the succinate minimal agar plates supplemented with an appropriate amino acid(s) at a concen-

tration of 1 mM (Table 2) and 12 mutants were auxotrophic for histidine or tryptophan (the His<sup>-</sup> or Trp<sup>-</sup> phenotype). Only one mutant, BT141, showed a leaky Trp<sup>-</sup> phenotype and formed very minute colonies on the minimal agar plates, and the addition of 1 mM tryptophan to the medium restored its growth to the wild-type rate. The remaining 22 auxotrophic mutants did not grow at all on the minimal agar plates.

**Mapping of transposon insertion sites on genome.** The TnMod-RTp' insert in a His<sup>-</sup> mutant, BT187, generated the 0.48- and 0.12-Mb *PacI* fragments with concomitant loss of the Chr I-derived 0.60-Mb *PacI* fragment (Fig. 3B, lanes 2 and 5). This mutant genome generated the 0.34-Mb and 0.16-Mb *SwaI* fragments instead of the 0.50-Mb *SwaI* fragment of the wild-type genome (Fig. 3B, lanes 6 and 9). The remaining four His<sup>-</sup> mutants showed restriction patterns indistinguishable from those of BT187, indicating that the transposon insertion sites in the five mutants were located close to one another within the 0.47-Mb *SwaI-PacI* fragment on Chr I (Fig. 1). The genome of the leaky Trp<sup>-</sup> mutant (BT141) gave rise to a doublet of the 135-kb *PacI* fragment instead of the 270-kb *PacI* fragment present in Chr II of ATCC 17616 (Fig. 3B, lanes 2 and 4). The genomes of the remaining six Trp<sup>-</sup> mutants (e.g., BT124) carried this 270-kb *PacI* fragment, and no apparent changes in the other *PacI* fragments were detected in comparisons of the genomes of these mutants with the wild-type genome (Fig. 3B, lanes 2 and 3). Loss of the wild-type 1.7-Mb *SwaI* fragment and novel generation of 1.2- and 0.53-Mb fragments in the six mutant genomes (Fig. 3B, lanes 6 and 7) indicated that all six transposon insertion sites were located close to one another at one end of the 2.2-Mb *PacI* fragment, which was adjacent to the 0.56-Mb *PacI* fragment on Chr I (Fig. 1).

BT122 and BT133 were auxotrophs for lysine (the Lys<sup>-</sup> phenotype) and arginine (the Arg<sup>-</sup> phenotype), respectively (Table 2). The *PacI* digestion of the BT122 and BT133 genomes resulted in the loss of the wild-type 1.4-Mb fragment, with concomitant generation of 1.3- and 0.10-Mb fragments and 1.1- and 0.30-Mb fragments, respectively (Fig. 3C, lanes 2, 3, and 5). Double digestion of the two mutant genomes with *PacI* and I-CeuI allowed their transposon insertions to map in the 0.44- and 0.96-Mb *PacI*-I-CeuI fragments, respectively, on Chr II (Fig. 1; Fig. 3C, lanes 8 to 10). In contrast, the transposon insertion in another Arg<sup>-</sup> mutant (BT129) was located within the region that was shared by the 2.2-Mb *PacI* and 1.2-Mb *SwaI* fragments on Chr I of ATCC 17616 (Fig. 3C, lanes 6 and 7) and generation of novel 0.25- and 0.95-Mb *SwaI* fragments from the BT129 genome indicated that the transposon insertion was located 0.25 Mb clockwise from the 0.50-Mb *SwaI* fragment (Fig. 1).

Similar PFGE analysis (data not shown) of the genomes of eight other auxotrophic mutants listed in Table 2 indicated that (i) their TnMod-RTp' insertion sites were distributed on Chr I and (ii) the insertion sites of the two aspartate-auxotrophic (Asp<sup>-</sup>) mutants were close to each other and those of the two isoleucine-auxotrophic (Ile<sup>-</sup>) mutants were also close to each other (Fig. 1).

**Detailed structure of the regions covering the transposon insertion sites.** The chromosomal DNA regions that covered the transposon insertion sites of the His<sup>-</sup>, Trp<sup>-</sup>, Arg<sup>-</sup>, and Lys<sup>-</sup> mutants (Table 2) were further investigated as follows. TnMod-RTp' carries the Tp' gene and the *oriV* region of plas-

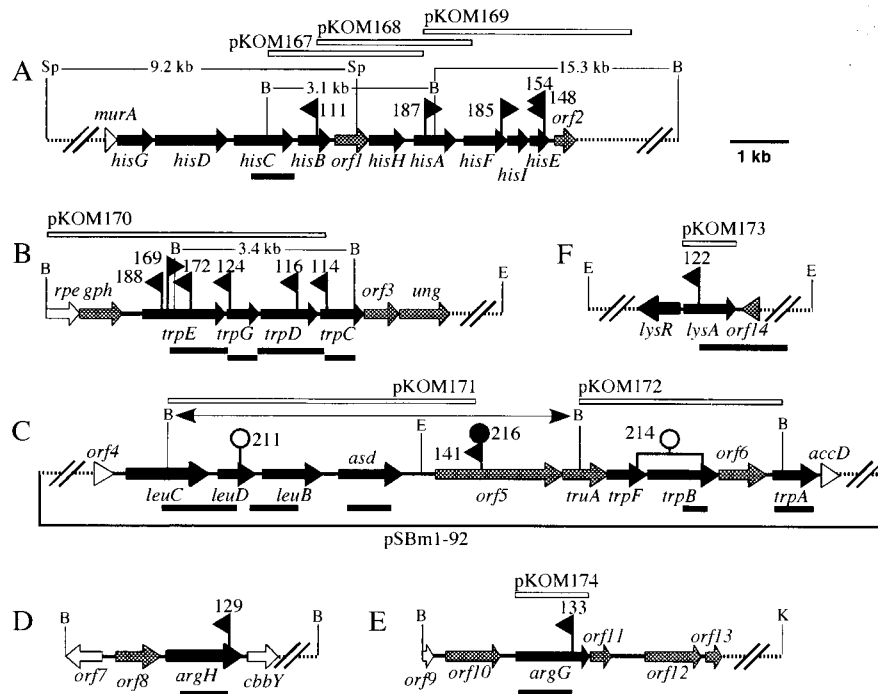


FIG. 4. Organization of the ATCC 17616 gene clusters covering the *TnMod-RTp'* insertion sites. The dashed lines indicate the regions not sequenced. Arrows indicate the deduced transcriptional directions of the genes: black arrows represent the genes directly involved in amino acid biosynthesis, shaded arrows represent the genes postulated not to be directly involved in amino acid biosynthesis, and open arrows and open triangles represent the 5'- or 3'-truncated genes not directly involved in amino acid biosynthesis. The flags represent the positions of the *TnMod-RTp'* insertion sites, and the mutant names (without the prefix BT) are indicated. The rightward and leftward directions of the flags represent the orientations of the *TnMod-RTp'* inserts such that the transposon-specified *Tp'* genes are located at the right and left ends (Fig. 2), respectively. The open and filled circles above the map in panel C indicate the positions of the pUC4K- and  $\Omega$ -Km-derived *Km<sup>r</sup>* genes, respectively, that were inserted into the ATCC 17616 genome to disrupt the wild-type allele, and the names of the resulting plasmids (without the prefix BT) are indicated. The open bars above the maps indicate the wild-type genomic regions on the pKOM series of plasmids, whereas the filled bars below the maps indicate the DNA fragments used as the probes for Southern hybridization analysis. The *Bam*HI fragment in pBTB141 is indicated by the double-headed arrow above the map in panel C. Abbreviations for restriction sites: B, *Bam*HI; E, *Eco*RI; K, *Kpn*I; and Sp, *Sph*I.

mid R6K but does not contain the *Eco*RI, *Bam*HI, or *Sph*I site (12). The plasmid containing the transposon and its flanking chromosomal regions were recovered by digestion of the genomic DNA with one of these enzymes, self-ligation, and subsequent selection of the *Tp<sup>r</sup>* transformants of an *E. coli* strain, JM109( $\lambda$ pir). The recovered plasmids were used to determine the sequences of the insertion sites and their flanking regions. Insertion of *Tn5* and its derivatives is well known to generate a 9-bp duplication of the target sequence (5), and all of the *TnMod-RTp'* insertion sites examined in the present study showed such 9-bp duplications (data not shown). To test whether the auxotrophic mutation was due to the *TnMod-RTp'* insertion, the recovered R6*KoriV*-driven plasmid was linearized by *Bam*HI or *Eco*RI digestion and inserted into the corresponding site of pEX18Tc (18) and the resulting plasmid was introduced into the ATCC 17616 cells to obtain the *Tp<sup>r</sup>* transformants. Among such transformants, those sensitive to Tc in which the donor *Tp<sup>r</sup>* marker was inserted into the wild-type genome by a homology-dependent double-crossover were chosen. These transformants showed auxotrophy identical to that of the original transposon-induced mutant, demonstrating that the auxotrophic phenotype was indeed due to the *TnMod-RTp'* insertion. This finding was also supported by the successful complementation of the mutation in the presence of

pBBR1MCS-based plasmids carrying the wild-type alleles. The functionality and copy numbers of the genes closely located to the *TnMod-RTp'* insert were investigated by (i) allelic exchange mutagenesis of the wild-type genome by the *Km<sup>r</sup>* gene, (ii) complementation by the pBBR1MCS-based plasmids carrying the wild-type alleles, and (iii) detection of homologous regions on the genome by Southern hybridization analysis under low-stringency conditions.

(i) **his genes.** All five *his* insertion mutations isolated in this study were located within a 4.1-kb segment on Chr I (Fig. 4A). Sequence analysis of the 8.5-kb region covering this segment revealed 11 genes in the following order: *hisG-hisD-hisC-hisB-orf1-hisH-hisA-hisF-hisI-hisE-orf2*. The *TnMod-RTp'* insertions were located in *hisB* (BT111), *hisA* (BT187), and *hisF* (BT185) and at the same position in *hisE* (BT148 and BT154) (Table 2), and these *his* insertion mutations were complemented by pKOM167, pKOM168, or pKOM169 (Fig. 4A). BLAST searches of the databases showed that *hisD* to *hisE*, the nine genes of ATCC 17616, had very high sequence identities (up to 84 and 89% in the nucleotide and amino acid sequences, respectively) to those of the *R. solanacearum* GMI1000 chromosome (Table 3) (31). Both bacteria shared the same order of these nine genes with the presence of an unknown gene, *orf1*, that was located between *hisB* and *hisH* (Fig. 4A). Involvement

TABLE 3. BLAST matches of the ATCC 17616 gene products<sup>a</sup>

Region and gene	Transcriptional direction	Product (no. of aa) <sup>b</sup>	Protein name and/or predicted function	Matching species <sup>c</sup>	Accession no.	No. (%) of amino acids with identity to those of matching species/total no. examined	No. (%) of amino acids with similarity to those of matching species/total no. examined
<i>his</i>							
<i>murA<sup>d</sup></i>	+	65	UDP-N-acetylglucosamine 1-carboxyvinyltransferase	<i>R. solanacearum</i>	AL646072	48/62 (77)	55/62 (88)
<i>hisG</i>	+	217	ATP phosphoribosyl transferase	<i>Neisseria meningitidis</i>	AE002508	140/205 (68)	163/205 (79)
<i>hisD</i>	+	438	Histidinol dehydrogenase	<i>R. solanacearum</i>	AL646072	344/437 (78)	374/437 (84)
<i>hisC</i>	+	364	Histidinol-phosphate aminotransferase	<i>R. solanacearum</i>	AL646072	219/359 (61)	259/359 (72)
<i>hisB</i>	+	195	Imidazoleglycerol-phosphate dehydratase	<i>R. solanacearum</i>	AL646072	173/194 (89)	183/194 (94)
<i>orf1</i>	+	206	Probable transmembrane protein	<i>R. solanacearum</i>	AL646072	131/206 (63)	160/206 (77)
<i>hisH</i>	+	213	Glutamine amidotransferase	<i>R. solanacearum</i>	AL646072	155/216 (71)	172/216 (78)
<i>hisA</i>	+	251	Phosphoribosylformimino-5-aminoimidazole carboxamide ribotide isomerase	<i>R. solanacearum</i>	AL646072	198/244 (81)	217/244 (88)
<i>hisF</i>	+	257	Imidazole glycerol phosphate synthase	<i>R. solanacearum</i>	AL646072	226/255 (88)	239/255 (93)
<i>hisI</i>	+	138	Phosphoribosyl-AMP cyclohydrolase	<i>R. solanacearum</i>	AL646072	95/127 (74)	112/127 (87)
<i>hisE</i>	+	121	Phosphoribosyl-ATP pyrophosphatase	<i>R. solanacearum</i>	AL646072	71/106 (66)	84/106 (78)
<i>orf2</i>	+	130	Probable transmembrane protein	<i>R. solanacearum</i>	AL646072	52/105 (49)	59/105 (55)
<i>trpEGDC</i>							
<i>rpe<sup>d</sup></i>	+	196	Ribulose-phosphate 3-epimerase	<i>R. solanacearum</i>	AL646072	145/202 (71)	162/202 (79)
<i>gph</i>	+	256	Phosphoglycolate phosphatase	<i>R. solanacearum</i>	AL646072	115/226 (50)	138/226 (60)
<i>trpE</i>	+	493	Anthranilate synthase component I	<i>R. solanacearum</i>	AL646072	355/466 (76)	395/466 (84)
<i>trpG</i>	+	195	Anthranilate synthase component II	<i>R. solanacearum</i>	AL646072	146/187 (78)	167/187 (89)
<i>trpD</i>	+	343	Anthranilate phosphoribosyltransferase	<i>R. solanacearum</i>	AL646072	282/345 (81)	311/345 (89)
<i>trpC</i>	+	261	Indole-3-glycerol phosphate synthase	<i>P. aeruginosa<sup>e</sup></i>	AE004500	160/260 (61)	186/260 (71)
<i>orf3</i>	+	208	Conserved hypothetical protein	<i>R. solanacearum</i>	AL646072	76/188 (40)	92/188 (48)
<i>ung</i>	+	301	Uracil-DNA glycosylase	<i>R. solanacearum</i>	AL646072	148/234 (63)	169/234 (71)
<i>leuCDB-trpFBA</i>							
<i>orf4<sup>d</sup></i>	+	106	Probable lipoprotein transmembrane	<i>R. solanacearum</i>	AL646083	51/93 (54)	64/93 (67)
<i>leuC</i>	+	477	3-Isopropylmalate dehydratase (large subunit)	<i>R. solanacearum</i>	AL646067	390/469 (83)	420/469 (89)
<i>leuD</i>	+	216	3-Isopropylmalate dehydratase (small subunit)	<i>R. solanacearum</i>	AL646067	185/216 (85)	200/216 (91)
<i>leuB</i>	+	355	3-Isopropylmalate dehydrogenase oxidoreductase	<i>R. solanacearum</i>	AL646067	303/354 (85)	321/354 (90)
<i>asd</i>	+	373	Aspartate-semialdehyde dehydrogenase	<i>P. aeruginosa<sup>e</sup></i>	AE004736	272/371 (73)	309/371 (82)
<i>orf5</i>	+	753	Probable transmembrane protein	<i>R. solanacearum</i>	AL646067	28/71 (39)	40/71 (55)
<i>truA</i>	+	270	tRNA pseudouridine synthase	<i>R. solanacearum</i>	AL646067	172/259 (66)	202/259 (77)
<i>trpF</i>	+	235	N-(5'-phosphoribosyl) anthranilate isomerase	<i>R. solanacearum</i>	AL646067	127/207 (61)	149/207 (71)
<i>trpB</i>	+	417	Tryptophan synthase (beta chain)	<i>R. solanacearum</i>	AL646067	347/400 (86)	375/400 (93)
<i>orf6</i>	+	283	Probable DNA-methyltransferase	<i>R. solanacearum</i>	AL646067	176/243 (72)	206/243 (84)
<i>trpA</i>	+	271	Tryptophan synthase (alpha chain)	<i>R. solanacearum</i>	AL646067	171/264 (64)	201/264 (75)
<i>accD<sup>d</sup></i>	+	87	Acetyl-CoA carboxylase (beta subunit)	<i>R. solanacearum</i>	AL646067	73/87 (83)	82/87 (93)
<i>argH</i>							
<i>orf7<sup>d</sup></i>	-	206	Putative biotin synthesis protein	<i>E. coli</i>	AP002550	109/202 (53)	136/202 (66)
<i>orf8</i>	+	269	Hypothetical protein	<i>Mesorhizobium loti</i>	AP002997	85/261 (32)	125/261 (47)
<i>argH</i>	+	469	Argininosuccinate lyase	<i>R. solanacearum</i>	AL646069	380/458 (82)	408/458 (88)
<i>cbbY<sup>d</sup></i>	+	164	CbbY family protein	<i>V. cholerae</i>	AE004353	65/166 (39)	91/166 (54)
<i>argG</i>							
<i>orf9<sup>d</sup></i>	+	68	Hypothetical protein	<i>Xanthomonas axonopodis</i>	AE011766	31/59 (52)	37/59 (62)
<i>orf10</i>	+	323	Probable transmembrane protein	<i>R. solanacearum</i>	AL646476	174/320 (54)	218/320 (67)
<i>orfG</i>	+	445	Argininosuccinate synthase	<i>N. meningitidis<sup>e</sup></i>	AE002561	348/438 (79)	383/438 (86)
<i>orf11</i>	+	126	Hypothetical protein	N <sup>f</sup>			
<i>orf12</i>	+	336	Hypothetical protein	N <sup>f</sup>			
<i>orf13</i>	+	102	Hypothetical protein	N <sup>f</sup>			
<i>lysA</i>							
<i>lysR</i>	-	315	Positive regulator for lys genes	<i>Yersinia pestis<sup>g</sup></i>	AE013919	147/304 (48)	203/304 (66)
<i>lysA</i>	+	412	Diaminopimelate decarboxylase	<i>Salmonella enterica</i> serovar Typhimurium	AE008838	268/407 (65)	319/407 (77)
<i>orf14</i>	-	61	Hypothetical protein	<i>Agrobacterium tumefaciens</i>	AE007963	25/44 (56)	33/44 (74)

<sup>a</sup> Standard analysis with the default parameters was carried out using the DDBJ/EMBL/GenBank databases available on March 5, 2003.

<sup>b</sup> Deduced length of amino acid residues.

<sup>c</sup> Matches to other *Burkholderia* strains are not listed because the print and online articles describing their genome sequences have not yet been published.

<sup>d</sup> The gene has not been fully sequenced.

<sup>e</sup> The product also showed high homology to the corresponding product of *R. solanacearum*. TrpC: identity, 66% (167/266); similarity, 71% (191/266). Asd: identity, 69% (261/373); similarity, 81% (307/373). ArgG: identity, 78% (347/443); similarity, 87% (387/443).

<sup>f</sup> N, significant homology was not detected in the databases.

<sup>g</sup> Homology to the *R. solanacearum* counterpart was not high (see text).

of *orf1* of ATCC 17616 in histidine biosynthesis was not investigated. The presence of *hisG* just upstream of *hisD* in the ATCC 17616 genome differed from that on the *R. solanacearum* genome, for which the position of the *hisG* gene remains unknown. However, the *hisG* sequence of ATCC 17616 showed very high homology (82% identity with a one-base gap) with the *R. solanacearum* DNA region that was located just upstream of *hisD*. Southern hybridization analysis (data not shown) indicated that the ATCC 17616 genome carried only one copy of *hisC* (Fig. 4A). This finding was in contrast with the presence in the *R. solanacearum* chromosome of an additional copy of the *hisC* gene (*hisC2*) not linked to the *his* gene cluster (31).

**(ii) *trp* genes.** All six *trp* insertion mutations mapped on Chr I were clustered within a 3.4-kb segment of a 7.5-kb sequenced fragment. This fragment contained the four *trp* genes in the following order: *trpE-trpG-trpD-trpC*. All of these genes were subjected to the insertion of TnMod-RTp' (Fig. 4B). The *trpE*, *trpD*, and *trpC* mutations were complemented by pKOM170. Each of the four *trp* gene products from ATCC 17616 also showed >61% amino acid sequence identity with the corresponding gene product encoded by the *R. solanacearum* chromosome (Table 3). The organization and structure of the genes other than the *trp* genes (Fig. 4B) were also highly conserved between the two bacteria, with the exception that a single open reading frame (ORF) (RSc2883) located between *trpG* and *trpD* in *R. solanacearum* (31) was absent in ATCC 17616. The *R. solanacearum* megaplasmid carried the second copy of *trpC* and *trpD* (*trpC2* and *trpD2*, respectively) (31). Our Southern hybridization analysis and disruption of the wild-type alleles of ATCC 17616 (data not shown) supported the idea of the presence of a single functional copy of the *trpEGDC* cluster on Chr I (Table 2 and Fig. 4B).

As described above, the leaky *trp* mutant (BT141) carried the transposon within the 0.27-Mb *PacI* fragment on Chr II (Fig. 3B). The 7.0-kb *Bam*HI fragment subjected to the transposon insertion (i.e., the chromosomal fragment on pBTB141) was sequenced, and BLAST searches of the databases revealed that the ORFs within this fragment did not have a clear match with any sequences that were directly or indirectly involved in tryptophan biosynthesis (Fig. 4C and Table 3). The *Bam*HI-linearized form of pBTB141 was inserted into pEX18Tc, and the resulting plasmid (pKOM152) (Fig. 4C and Table 1) was used to introduce the BT141-specified TnMod-RTp' insert into the ATCC 17616 genome by a homology-dependent double-crossover event. The resulting strain showed the same leaky Trp<sup>-</sup> phenotype as that exhibited by BT141, supporting the assumption that the leaky phenotype of BT141 was the result of the insertion of the transposon in *orf5*.

A pair of degenerated primers were designed based on the conserved amino acid sequences of the TrpB proteins in various bacterial species, and the internal 360-bp fragment of the ATCC 17616 *trpB* gene was amplified by PCR. One cosmid (pSBm1-92) hybridized with this PCR product carried, in addition to the pBTB141-loaded chromosomal region, a DNA region that was located downstream of *orf5* (Fig. 4C). Sequence analysis and subsequent database searches strongly suggested that this region carried the *trpF*, *trpB*, and *trpA* genes (Table 3). Disruption of the ATCC 17616 *trpF* and *trpB* genes by insertion of the pKOM157-derived Km<sup>r</sup> gene (Table 1)

conferred the Trp<sup>-</sup> phenotype on the resulting mutant (BT214), and Southern hybridization analysis using a portion of the *trpA* gene and the PCR product of the *trpB* gene as the probes (data not shown) showed a single-copy state of both genes on the genome (Fig. 4C). These results indicated that the *trpB* and *trpF* genes were indeed functional. The three Trp proteins of ATCC 17616 also showed very high homology with the respective proteins of *R. solanacearum* (Table 3), and the gene organization of the *truA-trpF-trpB-orf6-trpA* region in ATCC 17616 (Fig. 4C) was also highly conserved on the *R. solanacearum* chromosome. Involvement of *orf6* in tryptophan biosynthesis was not investigated. A plausible operon structure of at least the four genes, *orf5* to *trpB*, was inferred by very tight clustering (i.e., overlapping of the stop and start codons) of these genes and the presence of a strong promoter sequence upstream of *orf5*. Strain BT216 (Table 1) differed from BT141 (ATCC 17616*orf5*::TnMod-RTp') in that the ΩKm cassette containing the transcriptional terminator sequence was added to the right end of the transposon (Fig. 4C). BT216 also showed the leaky Trp<sup>-</sup>. This leaky phenotype of BT141 and BT216 was complemented by the introduction of pKOM173, which carried the wild-type *trpFB* genes but not *orf5*, indicating that the putative *orf5* product in itself was not responsible for the leaky phenotype of BT141 and BT216.

**(iii) Genes located close to *trpFBA* genes on Chr II.** The 5.3-kb chromosomal region upstream of *orf5* carried the putative *leuCDB* and *asd* genes (Fig. 4C). The last gene encodes aspartate-semialdehyde dehydrogenase, which produces in many bacterial species a cell-wall precursor, meso-diaminopimelate, as well as L-aspartate 4-semialdehyde, a common precursor for the biosynthesis of several amino acids (10). The gene organization of the *leuCDB-asd* region also showed high resemblance to the corresponding region on the *R. solanacearum* chromosome (Table 3). Southern hybridization analysis (data not shown) indicated that the ATCC 17616 genome possessed a single copy of the *leuCDB* gene cluster and the *asd* gene (Fig. 4C). Disruption of the wild-type *leuD* allele of ATCC 17616 by insertion of the pKOM154-loaded Km<sup>r</sup> gene led to the generation of the mutant auxotrophic for leucine (BT211), and the BT211 derivative carrying pKOM171 (Fig. 4C) showed prototrophy. These results indicated that the *leuD* gene was indeed functional.

**(iv) *arg* and *lys* genes.** The Chr I- and Chr II-loaded TnMod-RTp' inserts in the two Arg<sup>-</sup> mutants, BT129 and BT133, respectively, were situated in the *argH* and *argG* genes, respectively, and each gene was neither followed nor preceded by the genes related to arginine biosynthesis (Fig. 4D and E). The Chr II-loaded transposon insert in the Lys<sup>-</sup> mutant, BT122, was located within *lysA* (Fig. 4F). Located adjacent to this gene was the putative *lysR* gene, and the two genes had a head-to-head organization with respect to their relative transcriptional directions. We did not investigate the functionality of the *lysR* gene. Disruption of the Chr II-loaded *argG* and *lysA* alleles of ATCC 17616 by the cloned TnMod-RTp' insertion mutations resulted in the generation of the Arg<sup>-</sup> and Lys<sup>-</sup> mutants, respectively. The introduction of pKOM174 into BT133 and pKOM173 into BT122 led to normal growth of the resulting strains on the minimal agar plates. Southern hybridization analysis (data not shown) also identified no structural homologues of *argG*, *argH*, or *lysA* on the ATCC 17616 genome

(Table 2 and Fig. 4). The ArgH and ArgG proteins revealed very high amino acid sequence identities (82 and 78%, respectively) to those encoded by the *R. solanacearum* chromosome (Table 3), whereas the LysA and LysR proteins showed much lower identities (34 and 32%, respectively). The other ORF products in the *argG* and *lysA* regions revealed no significant homology with those encoded by *R. solanacearum* and its related species.

## DISCUSSION

In this study, the TnMod-RTp'-inserted mutations which were auxotrophic for various amino acids were isolated from *B. multivorans* ATCC 17616 (Table 2) and such mutation sites were found to be distributed on Chr I and Chr II (Fig. 1 and 4). The same strain has been previously used by Cheng and Lessie (8) to demonstrate the positions of their *arg*, *his*, and *ile* mutations on Chr I and a *lys* mutation on Chr II. Although these mutations have not been characterized in detail, their positions on the genome map matched those of our mutations that exhibited similar auxotrophic phenotypes. Use of the transposon-inserted mutations led to further identification of the 24 auxotrophic genes (Fig. 4 and Table 3), and the knockout mutagenesis, complementation tests, and Southern hybridization analysis clarified that such genes had no other functional or structural homologues on the other regions of the genome. Many bacterial species require nine *his* genes (*hisA* to *hisI*) and seven *trp* genes (*trpA* to *trpG*) for the complete biosynthesis of histidine and tryptophan, respectively, and all of these structural genes were identified on the ATCC 17616 genome. While all of the nine *his* genes were clustered on Chr I, the *trpEGDC* and *trpFBA* clusters were located on Chr I and Chr II, respectively. Although not all of the genes necessary for the complete biosynthesis of arginine, leucine, and lysine were identified in this study, we demonstrated the single-copy state of the functional *argG*, *leuCDB*, and *lysA* genes on Chr II. The amino acid biosynthetic genes we detected on Chr I and Chr II did not reveal any significant differences with respect to their G+C content and codon usage.

Among the bacterial strains of which the complete genome sequences have been published in print or online articles, *R. solanacearum* GMI1000, a strain very closely related to *B. multivorans* from a phylogenetical point of view, showed the highest homology to ATCC 17616 with regard to our identified auxotrophic genes (31). Remarkable similarity between the two bacteria was also found in the organization of the *his*, *trpEGDC*, and *leuCDB-trpFBA* clusters (Fig. 4) as well as in the presence of large noncoding regions (e.g., the regions flanking the *asd* gene; Fig. 4C). However, *R. solanacearum* was found to carry the three clusters and the *argH*, *argG*, and *lysA* genes on the same chromosome but not on the megaplasmid. Some of the auxotrophic genes of *R. solanacearum* were reported to be duplicated (or triplicated), and their second and/or third copies (whose functionality remains to be investigated) were located on the chromosome (in the case of *hisC* and *trpD*) or on the megaplasmid (in the case of *leuB*, *trpC*, and *trpD*). Similar distribution of duplicated (or triplicated) copies of certain auxotrophic genes in different replicons has been observed in other multichromosomal bacteria such as *Agrobacterium tumefaciens*, *Sinorhizobium meliloti*, and *Vibrio cholerae* (17, 31, 40).

The multichromosomal bacteria in certain cases carry a few auxotrophic genes only on the secondary chromosomes. Examples of such genes include *trpB* and *trpF* in *R. sphaeroides*, *metB* and *metE* in *R. solanacearum*, *metF* and *asd* in *Leptospira interrogans*, *metE* and *lysC* in *A. tumefaciens*, and several genes in *Deinococcus radiodurans* and two *Brucella* strains, *B. melitensis* and *B. suis* (6, 11, 16, 23, 28, 31, 39, 42). However, it should be noted that the functionality of these genes has not yet been investigated experimentally except in the case of the two *trp* genes of *R. sphaeroides*. Furthermore, these genes are typically not clustered with their related genes. Therefore, the *B. multivorans* ATCC 17616 genome differs considerably from those of *R. solanacearum* and other multichromosomal bacteria in that (i) all of the auxotrophic genes thus far examined exist in a single copy within the genome and (ii) many auxotrophic genes (i.e., at least those in the *leuCDB-trpFBA* region and the *argG* and *lysA* genes and most probably many other genes as well) are present only on Chr II. It is of interest that the flanking regions of the *argH* gene on Chr I and those of the *argG* and *lysA* genes on Chr II did not reveal structural similarities to those of *R. solanacearum* (Table 3). Additional sequence analysis of ATCC 17616 should reveal the extent of the differences between the two genomes.

A unique structural property of the ATCC 17616 genome that was also associated with the *R. solanacearum* genome was that the apparently unrelated ORFs were tightly linked to the auxotrophic gene clusters. This was exemplified by *murA*, *orf1*, *orf3*, *orf5*, and *truA*; overlapping of the predicted stop and start codons of the neighboring genes was observed in the *murA-hisG*, *orf1-hisH*, *trpC-orf3*, and *orf5-truA-trpF-trpB* regions. Although the roles of *orf1*, *orf3*, and *orf5* in histidine and tryptophan biosynthesis were not elucidated in this study, the leaky Trp<sup>-</sup> phenotype of the *orf5::TnMod-RTp'* mutant (BT141) remained unchanged after the addition of a transcriptional terminator sequence at the right end of the transposon (in BT216) (Fig. 4C). The leaky Trp<sup>-</sup> phenotype of BT141 and BT216 in the absence of tryptophan was complemented by pKOM173, which carried the wild-type alleles of *trpFB* genes but not that of *orf5*. This finding suggested that the normal growth of the cells without tryptophan required strong transcription from the promoter located upstream of *orf5*.

Based on the nearly random mode of insertion of Tn5 into various replicons (5), we anticipated that the TnMod-RTp' insertion mutants carrying the transposons on Chr III occupied a one-seventh [0.9 Mb/(0.9 + 2.5 + 3.4) Mb] proportion in the mutant library. No such mutants were found among more than 100 randomly chosen transposon-inserted derivatives. Although the reasons for our failure to obtain such mutants are unknown at present, Chr III might possess a unique structure that does not easily permit the maintenance of the TnMod-RTp' insert. Since the ATCC 17616 cells maintained Chr III under various laboratory growth conditions, this chromosome might play an important role in the propagation of host cells. To determine whether or not such an influence exists, we are currently analyzing the Chr III-derived DNA fragments present on some of the cosmid clones.

A pathogenic *B. cepacia* genomovar III strain, J2315, and a *B. fungorum* (formerly *B. cepacia*) strain, LB400, carry three circular chromosomes (24). Determination of the genome sequence of the former strain was completed in January 2003,

and that of the latter strain is now in progress. Comparison with these two strains revealed that the ATCC 17616 auxotrophic genes identified in this study were highly homologous to those of *B. cepacia* J2315 (94 and 97% identity with the nucleotide and amino acid sequences, respectively) (NC\_004503) and to those of *B. fungorum* LB400 (88 and 93%, respectively) (NZ\_AAAC0100000). The organizations of the six ATCC 17616 gene clusters shown in Fig. 4 were also conserved in the two *Burkholderia* strains. In *B. cepacia* J2315, the genome of which consists of 3.9-, 3.2-, and 0.9-Mb chromosomes (ftp://ftp.sanger.ac.uk/pub/pathogens/bc/), it was found that the *argH*, *his*, and *trpEGDC* regions are located on the 3.9-Mb chromosome and the *argG*, *leuCDB-trpFBA*, and *lysA* regions are located on the 3.2-Mb chromosome. This finding indicated that the six auxotrophic gene regions on the *B. multivorans* ATCC 17616 genome (Fig. 1 and 4) were similarly distributed on the *B. cepacia* J2315 genome. However, the 3.9-Mb chromosome of *B. cepacia* carried both the *dnaK* and *dnaA* genes in the following order: *dnaK-his* region-*trpEGDC-dnaA*. This is a striking difference from the genome of our *B. multivorans* strain, in which (i) the *dnaA* and *dnaK* genes were located on Chr I and Chr II, respectively, and (ii) the former gene was situated between the *his* and *trpEGDC* regions (our unpublished data). More detailed comparative analysis of the two bacteria would be necessary to determine the various distributions of other genes. Such investigations should provide further insight into the molecular mechanisms of the differentiation of bacterial genomes.

#### ACKNOWLEDGMENTS

This work was supported by the Research for the Future Programs of the Japan Society for the Promotion of Science and a Grant-in-Aid for Scientific Research from the Ministry of Education, Culture, Sports, Science and Technology, Japan.

Preliminary sequence data for the *B. fungorum* LB400 and *B. cepacia* J2315 genomes were obtained from The DOE Joint Genome Institute (JGI) at [http://www.jgi.doe.gov/JGI\\_microbial/html/burkholderia/burk\\_homepage.html](http://www.jgi.doe.gov/JGI_microbial/html/burkholderia/burk_homepage.html) and from the Sanger Institute at <ftp://ftp.sanger.ac.uk/pub/pathogens/bc/>, respectively.

#### REFERENCES

- Allardet-Servent, A., S. Michaux-Charachon, E. Jumas-Bilak, L. Karayan, and M. Ramuz. 1993. Presence of one linear and one circular chromosome in the *Agrobacterium tumefaciens* C58 genome. *J. Bacteriol.* **175**:7869–7874.
- Amann, R. L., W. Ludwig, and K. H. Schleifer. 1995. Phylogenetic identification and *in situ* detection of individual microbial cells without cultivation. *Microbiol. Rev.* **59**:143–169.
- Ausubel, F. M., R. Brent, E. R. Kingston, D. D. Moore, G. J. Seidman, A. J. Smith, and K. Struhl. 1991. Current protocols in molecular biology. John Wiley & Sons, New York, N.Y.
- Barsomian, G., and T. G. Lessie. 1986. Replicon fusions promoted by insertion sequences on *Pseudomonas cepacia* plasmid pTGL6. *Mol. Gen. Genet.* **204**:273–280.
- Berg, D. E. 1989. Transposon Tn5, p. 185–210. In D. E. Berg and M. M. Howe (ed.), *Mobile DNA*. American Society for Microbiology, Washington, D.C.
- Bourhy, P., and I. Saint-Girons. 2000. Localization of the *Leptospira interrogans metF* gene on the CII secondary chromosome. *FEMS Microbiol. Lett.* **191**:259–263.
- Capela, D., F. Barloy-Hubler, J. Gouzy, G. Bothe, F. Ampe, J. Batut, P. Boistard, A. Becker, M. Boutry, E. Cadieu, S. Dréano, S. Gloux, T. Godrie, A. Goffeau, D. Kahn, E. Kiss, V. Lelaure, D. Masuy, T. Pohl, D. Portetelle, A. Pühler, B. Purnelle, U. Ramsperger, C. Renard, P. Thébault, M. Vandenberg, S. Weidner, and F. Galibert. 2001. Analysis of the chromosome sequence of the legume symbiont *Sinorhizobium meliloti* strain 1021. *Proc. Natl. Acad. Sci. USA* **98**:9877–9882.
- Cheng, H. P., and T. G. Lessie. 1994. Multiple replicons constituting the genome of *Pseudomonas cepacia* 17616. *J. Bacteriol.* **176**:4034–4042.
- Coenye, T., P. Vandamme, J. R. Govan, and J. J. LiPuma. 2001. Taxonomy and identification of the *Burkholderia cepacia* complex. *J. Clin. Microbiol.* **39**:3427–3436.
- Cohen, G. N., and I. Saint-Girons. 1987. Biosynthesis of threonine, lysine, and methionine, p. 429–444. In F. C. Neidhardt, J. L. Ingraham, K. B. Low, B. Magasanik, M. Schaechter, and H. E. Umbarger (ed.), *Escherichia coli and Salmonella typhimurium: cellular and molecular biology*. American Society for Microbiology, Washington, D.C.
- DelVecchio, V. G., V. Kapatral, R. J. Redkar, G. Patra, C. Mujer, T. Los, N. Ivanova, I. Anderson, A. Bhattacharyya, A. Lykidis, G. Reznik, L. Jablonski, N. Larsen, M. D'Souza, A. Bernal, M. Mazur, E. Goltsman, E. Selkov, P. H. Elzer, S. Hagijs, D. O'Callaghan, J. J. Letesson, R. Haselkorn, N. Kyrpides, and R. Overbeek. 2002. The genome sequence of the facultative intracellular pathogen *Brucella melitensis*. *Proc. Natl. Acad. Sci. USA* **99**:443–448.
- Dennis, J. J., and G. J. Zylstra. 1998. Plasposons: modular self-cloning minitransposon derivatives for rapid genetic analysis of gram-negative bacterial genomes. *Appl. Environ. Microbiol.* **64**:2710–2715.
- Fellay, R., J. Frey, and H. Krisch. 1987. Interposon mutagenesis of soil and water bacteria: a family of DNA fragments designed for *in vitro* insertional mutagenesis of gram-negative bacteria. *Gene* **52**:147–154.
- Gaffney, T. D., and T. G. Lessie. 1987. Insertion-sequence-dependent rearrangements of *Pseudomonas cepacia* plasmid pTGL1. *J. Bacteriol.* **169**:224–230.
- Galibert, F., T. M. Finan, S. R. Long, A. Pühler, P. Abola, F. Ampe, F. Barloy-Hubler, M. J. Barnett, A. Becker, P. Boistard, G. Bothe, M. Boutry, L. Bowser, J. Buhrmester, E. Cadieu, D. Capela, P. Chain, A. Cowie, R. W. Davis, S. Dréano, N. A. Federspiel, R. F. Fisher, S. Gloux, T. Godrie, A. Goffeau, B. Golding, J. Gouzy, M. Gurjal, I. Hernandez-Lucas, A. Hong, L. Huizar, R. W. Hyman, T. Jones, D. Kahn, M. L. Kahn, S. Kalman, D. H. Keating, E. Kiss, C. Komp, V. Lelaure, D. Masuy, C. Palm, M. C. Peck, T. M. Pohl, D. Portetelle, B. Purnelle, U. Ramsperger, R. Surzycki, P. Thebault, M. Vandenberg, F. J. Vorholter, S. Weidner, D. H. Wells, K. Wong, K. C. Yeh, and J. Batut. 2001. The composite genome of the legume symbiont *Sinorhizobium meliloti*. *Science* **293**:668–672.
- Goodner, B., G. Hinkle, S. Gattung, N. Miller, M. Blanchard, B. Qurollo, B. S. Goldman, Y. Cao, M. Askenazi, C. Halling, L. Mullin, K. H. Houmli, J. Gordon, M. Vaudin, O. Iartchouk, A. Epp, F. Liu, C. Wollam, M. Allinger, D. Doughty, C. Scott, C. Lappas, B. Markelz, C. Flanagan, C. Crowell, J. Gurson, C. Lomo, C. Sear, G. Strub, C. Cielo, and S. Slater. 2001. Genome sequence of the plant pathogen and biotechnology agent *Agrobacterium tumefaciens* C58. *Science* **294**:2323–2328.
- Heidelberg, J. F., J. A. Eisen, W. C. Nelson, R. A. Clayton, M. L. Gwinn, R. J. Dodson, D. H. Haft, E. K. Hickey, J. D. Peterson, L. Umayam, S. R. Gill, K. E. Nelson, T. D. Read, H. Tettelin, D. Richardson, M. D. Ermolaeva, J. Vamathevan, S. Bass, H. Qin, I. Dragoi, P. Sellers, L. McDonald, T. Utterback, R. D. Fleishmann, W. C. Nierman, and O. White. 2000. DNA sequence of both chromosomes of the cholera pathogen *Vibrio cholerae*. *Nature* **406**:477–483.
- Hoang, T. T., R. R. Karkhoff-Schweizer, A. J. Kutchma, and H. P. Schweizer. 1998. A broad-host-range F<sub>1</sub>-FRT recombination system for site-specific excision of chromosomally-located DNA sequences: application for isolation of unmarked *Pseudomonas aeruginosa* mutants. *Gene* **212**:77–86.
- Honeycutt, R. J., M. McClelland, and B. W. Sobral. 1993. Physical map of the genome of *Rhizobium meliloti* 1021. *J. Bacteriol.* **175**:6945–6952.
- Kovach, M. E., P. H. Elzer, D. S. Hill, G. T. Robertson, M. A. Farris, R. M. Roop II, and K. M. Peterson. 1995. Four new derivatives of the broad-host-range cloning vector pBBR1MCS, carrying different antibiotic-resistance cassettes. *Gene* **166**:175–176.
- Lessie, T. G., W. Hendrickson, B. D. Manning, and R. Devereux. 1996. Genomic complexity and plasticity of *Burkholderia cepacia*. *FEMS Microbiol. Lett.* **144**:117–128.
- Liu, S. L., A. Hessel, and K. E. Sanderson. 1993. Genomic mapping with I-CeuI, an intron-encoded endonuclease specific for genes for ribosomal RNA, in *Salmonella* spp., *Escherichia coli*, and other bacteria. *Proc. Natl. Acad. Sci. USA* **90**:6874–6878.
- Mackenzie, C., A. E. Simmons, and S. Kaplan. 1999. Multiple chromosomes in bacteria. The yin and yang of *trp* gene localization in *Rhodobacter sphaeroides* 2.4.1. *Genetics* **153**:525–538.
- Madden, T. L., R. L. Tatusov, and J. Zhang. 1996. Applications of network BLAST server. *Methods Enzymol.* **266**:131–141.
- Michaux, S., J. Paullisson, M. J. Carles-Nurit, G. Bourg, A. Allardet-Servent, and M. Ramuz. 1993. Presence of two independent chromosomes in the *Brucella melitensis* 16M genome. *J. Bacteriol.* **175**:701–705.
- Nichols, B. P. 1996. Evolution of genes and enzymes of tryptophan biosynthesis, p. 2638–2648. In F. C. Neidhardt, R. Curtiss III, J. L. Ingraham, E. C. Lin, K. B. Low, B. Magasanik, W. S. Reznikoff, M. Riley, M. Schaechter, and H. E. Umbarger (ed.), *Escherichia coli and Salmonella: cellular and molecular biology*, 2nd ed., vol. 2. American Society for Microbiology, Washington, D.C.
- Parke, J. L., and D. Gurian-Sherman. 2001. Diversity of the *Burkholderia cepacia* complex and implications for risk assessment of biological control strains. *Annu. Rev. Phytopathol.* **39**:225–258.
- Paulsen, I. T., R. Seshadri, K. E. Nelson, J. A. Eisen, J. F. Heidelberg, T. D.

- Read, R. J. Dodson, L. Umayam, L. M. Brinkac, M. J. Beanan, S. C. Daugherty, R. T. Deboy, A. S. Durkin, J. F. Kolonay, R. Madupu, W. C. Nelson, B. Ayodeji, M. Kraul, J. Shetty, J. Malek, S. E. Van Aken, S. Riedmuller, H. Tettelin, S. R. Gill, O. White, S. L. Salzberg, D. L. Hoover, L. E. Lindler, S. M. Halling, S. M. Boyle, and C. M. Fraser. 2002. The *Brucella suis* genome reveals fundamental similarities between animal and plant pathogens and symbionts. *Proc. Natl. Acad. Sci. USA* **99**:13148–13153.
29. Ramos-Díaz, M. A., and J. L. Ramos. 1998. Combined physical and genetic map of the *Pseudomonas putida* KT2440 chromosome. *J. Bacteriol.* **180**:6352–6363.
30. Rodley, P. D., U. Romling, and B. Tümmler. 1995. A physical genome map of the *Burkholderia cepacia* type strain. *Mol. Microbiol.* **17**:57–67.
31. Salanoubat, M., S. Genin, F. Artiguenave, J. Gouzy, S. Mangenot, M. Arlat, A. Billault, P. Brottier, J. C. Camus, L. Cattolico, M. Chandler, N. Choisine, C. Claudel-Renard, S. Cunnac, N. Demange, C. Gaspin, M. Lavie, A. Moisan, C. Robert, W. Saurin, T. Schiex, P. Siguier, P. Thebault, M. Whalen, P. Wincker, M. Levy, J. Weissenbach, and C. A. Boucher. 2002. Genome sequence of the plant pathogen *Ralstonia solanacearum*. *Nature* **415**:497–502.
32. Sambrook, J., and D. W. Russell. 2001. *Molecular cloning: a laboratory manual*, 3rd ed. Cold Spring Harbor Laboratory Press, New York, N.Y.
33. Schweizer, H. P. 1992. Allelic exchange in *Pseudomonas aeruginosa* using novel ColE1-type vectors and a family of cassettes containing a portable *oriT* and the counter-selectable *Bacillus subtilis sacB* marker. *Mol. Microbiol.* **6**:1195–1204.
34. Simon, R., U. Priefer, and A. Pühler. 1983. A broad host range mobilization system for in vivo genetic engineering: transposon mutagenesis in gram negative bacteria. *Bio/Technology* **1**:784–791.
35. Suwanto, A., and S. Kaplan. 1989. Physical and genetic mapping of the *Rhodobacter sphaeroides* 2.4.1 genome: presence of two unique circular chromosomes. *J. Bacteriol.* **171**:5850–5859.
36. Taylor, L. A., and R. E. Rose. 1988. A correction in the nucleotide sequence of the Tn903 kanamycin resistance determinant in pUC4K. *Nucleic Acids Res.* **16**:358.
37. Trucksis, M., J. Michalski, Y. K. Deng, and J. B. Kaper. 1998. The *Vibrio cholerae* genome contains two unique circular chromosomes. *Proc. Natl. Acad. Sci. USA* **95**:14464–14469.
38. Vandamme, P., B. Holmes, M. Vancanneyt, T. Coenye, B. Hoste, R. Coopman, H. Revets, S. Lauwers, M. Gillis, K. Kersters, and J. R. Govan. 1997. Occurrence of multiple genomovars of *Burkholderia cepacia* in cystic fibrosis patients and proposal of *Burkholderia multivorans* sp. nov. *Int. J. Syst. Bacteriol.* **47**:1188–1200.
39. White, O., J. A. Eisen, J. F. Heidelberg, E. K. Hickey, J. D. Peterson, R. J. Dodson, D. H. Haft, M. L. Gwinn, W. C. Nelson, D. L. Richardson, K. S. Moffat, H. Qin, L. Jiang, W. Pamphile, M. Crosby, M. Shen, J. J. Vamathevan, P. Lam, L. McDonald, T. Utterback, C. Zalewski, K. S. Makarova, L. Aravind, M. J. Daly, C. M. Fraser, et al. 1999. Genome sequence of the radioresistant bacterium *Deinococcus radiodurans* R1. *Science* **286**:1571–1577.
40. Yamaichi, Y., T. Iida, K. S. Park, K. Yamamoto, and T. Honda. 1999. Physical and genetic map of the genome of *Vibrio parahaemolyticus*: presence of two chromosomes in *Vibrio* species. *Mol. Microbiol.* **31**:1513–1521.
41. Yanisch-Perron, C., J. Vieira, and J. Messing. 1985. Improved M13 phage cloning vectors and host strains: nucleotide sequences of the M13mp18 and pUC19 vectors. *Gene* **33**:103–119.
42. Zuerner, R. L., J. L. Herrmann, and I. Saint-Girons. 1993. Comparison of genetic maps for two *Leptospira interrogans* serovars provides evidence for two chromosomes and intraspecies heterogeneity. *J. Bacteriol.* **175**:5445–5451.